Cosmic Research, Vol. 38, No. 6, 2000, pp. 527–539. Translated from Kosmicheskie Issledovaniya, Vol. 38, No. 6, 2000, pp. 563–576.

The Earth's Magnetosphere Response to Solar Wind Events according to the INTERBALL Project Data*

Yu. I. Yermolaev, G. N. Zastenker, and N. S. Nikolaeva

Space Research Institute, Russian Academy of Sciences, Profsoyuznaya ul. 84/32, Moscow, 117810 Russia

Received August 10, 2000

Abstract—The results of studying the interaction of two types of the solar wind (magnetic clouds and solar wind of extremely low density) with the Earth's magnetosphere are discussed. This study is based of the INTERBALL space project measurements and on the other ground-based and space observations. For moderate variations of the solar wind and interplanetary magnetic field (IMF) parameters, the response of the magnetosphere is similar to its response to similar changes in the absence of magnetic clouds and depends on a previous history of IMF variations. Extremely large density variations on the interplanetary shocks, and on leading and trailing edges of the clouds result in a strong deformation of the magnetosphere, in large-scale motion of the geomagnetic tail, and in the development of magnetic substorms and storms. The important consequences of these processes are: (1) the observation of regions of the magnetosphere and its boundaries at great distances from the average location; (2) density and temperature variations in the outer regions of the magnetosphere; (3) multiple crossings of geomagnetic tail boundaries by a satellite; and (4) bursty fluxes of electrons and ions in the magnetotail, auroral region, and the polar cap. Several polar activations and substorms can develop during a single magnetic cloud arrival; a greater number of these events are accompanied, as a rule, by the development of a stronger magnetic storm. A gradual, but very strong, decrease of the solar wind density on May 10–12, 1999, did not cause noticeable change of geomagnetic indices, though it resulted in considerable expansion of the magnetosphere.

INTRODUCTION

The solar wind is one of basic agents transferring the energy from the Sun to the Earth's magnetosphere. Therefore, one of the basic issues of solar–terrestrial physics is the question, which magnetosphere responses are caused by different changes in the interplanetary medium [1]. This issue has been discussed thoroughly enough in the literature (see, e.g., the collection of papers [2]). It was shown there, that, under quasi-stationary conditions, the existence of the southward component of the interplanetary magnetic field (IMF) promotes the energy input into the magnetosphere and its accumulation in the magnetotail. Then, upon reaching some particular level, this energy, due to external, though small impact (such as a jump of pressure or magnetic field in the solar wind) or due to internal dynamics of the magnetosphere, can begin to release as a rearrangement of current systems and as plasma acceleration or heating, which results in the development of magnetospheric disturbances, such as magnetic storms and substorms.

However, there exist rather strong solar wind disturbances, whose influence on the Earth's magnetosphere is not sufficiently studied yet. The main sources of such dynamic phenomena in the solar wind, as magnetic clouds (MC) and the interplanetary shocks (IS), are coronal mass ejections (see reviews [3, 4] and the special issue of *Geophys. Res. Lett.*, 1998, no. 14).

The geomagnetic indices, used for the quantitative estimation of magnetic storms (D_{st}, for example), well enough correlate with arrivals of magnetic clouds, if the correlation is investigated over time scales of about 10 h [4, 5]. The substorms and others auroral disturbances have characteristic times of the order of several tens of minutes, and they should be compared not with the magnetic cloud as a whole, but with its separate structures and boundaries, such as the shock wave in front of MC, the leading and trailing edges (LE and TE) of MC, the IS in front of TE, the jumps of plasma pressure, the changes of IMF magnitude and orientation. In addition, the motion of various magnetosphere regions and the change of their characteristics under these unusual conditions are of interest as well. Such an analysis for a small number of most remarkable events has already been initiated on the basis of observations in the multi-satellite INTERBALL project [6–8], and here we summarize the results of our analysis on the basis of a greater statistics. Alongside, we consider the influence on the Earth's magnetosphere of an extremely rare phenomenon in the solar wind. This phenomenon was observed on May 10–12, 1999, when the solar wind (SW) plasma density gradually decreased 20 times as compared to its average value [9].

* This paper is prepared on the basis of a report presented at the 5th International Conference on Substorms, May 16–20, 2000, St. Petersburg, Russia.

0010-9525/00/3806-0527$25.00 © 2000 MAIK "Nauka / Interperiodica"

Table 1. Magnetic clouds according to observations on different spacecraft

No.	Date	Durations, h		Space regions according to *INTERBALL-1*	Conditions in SW
		MC	(+IS)		
	1995				
1	Oct. 18–19	28	(+8)	MS/MSH/MS	Variations of B_z
	1996				
2	Dec. 24–25	39	(+10)	MS/MSH/MS	Jumps of P
	1997				
3	Jan. 10–11	23	(+4)	MS/MSH/MS	SW with $N \sim 150$ cm^{-3}
4	Feb. 9–11	41	(+14)	SW/MSH/MS/MSH/SW	$B_z < 0$
5	Apr. 10–11	22	(+9)	SW	Changes of B_z
6	Apr. 21–23	43	(+1)	SW	Jumps of P
7	May 15–16	46	(+4)	SW	Changes of B_z
8	June 8–9	24	(+3)	MS/MSH/SW	Jumps of P
9	June 19	10	(+6)	SW	Quiet SW
10	July 15–16	45	(+6)	SW	$B_z < 0$
11	Aug. 3–4	13	(+4)	SW/ MSH/SW	Quiet SW
12	Sept. 3	12	(+10)	SW/MSH/MS	Jumps of B_z
13	Sept. 18–20	56	(+4)	MS/MSH/MS	Jumps of B_z
14	Sept. 21	5	(+5)	MSH	Jumps of P
15	Sept. 21–22	19	(+3)	MSH/SW	Jumps of P
	1997				
16	Oct. 1–2	42	(+4)	MS/MSH/MS	–
17	Oct. 10–12	45	(+5)	MSH	Jumps of P
18	Nov. 7–8	24	(+7)	MS	Variations of P and B_z
19	Nov. 22–23	18	(+10)	MS	$B_z < 0$
20	Dec. 10–11	15	(+16)	MS	Jumps of B_z
21	Dec. 30–31	25	(+7)	MS	Jumps of P and B_z
	1998				
22	Jan. 7–8	29	(+14)	MS	Jumps of B_z
23	Feb. 4–5	41	(+17)	MSH/MS	Jumps of P
24	Feb. 17–18	14	(+16)	MS/MSH	Jumps of P and B_z
25	Mar. 4–5	30	(+4)	MS/MSH/SW	Jumps of B_z
26	May 2–3	?	(+14)	SW	$B_z < 0$
27	May 4–5	15	(+9)	SW/MSH	Jumps of B_z
28	June 2	8	?	SW	Quiet SW
29	June 24–25	35	(+4)	SW	Jumps of P
30	Sept. 25–26	29	(+7)	MSH/MS	Jumps of P
	Average	27	(+8)		

MAGNETIC CLOUDS AND "WEAK" SOLAR WIND

For the analysis of interplanetary conditions we use the key parameters of plasma and magnetic field, which have been measured by the *WIND* and, in some cases, by the other spacecraft (*SOHO* and *IMP-8*). As an example of MC, we consider the well-known event on January 10–11, 1997, where the MC arrival to the Earth has resulted in a strong magnetosphere disturbance and in the failure of the *Telstar-401* communication satellite. This MC (see Fig. 1 and [3]) has both the features common with other MCs (the shock wave in front of MC, the strong and slowly rotating magnetic field B, the low density N and temperature T between density

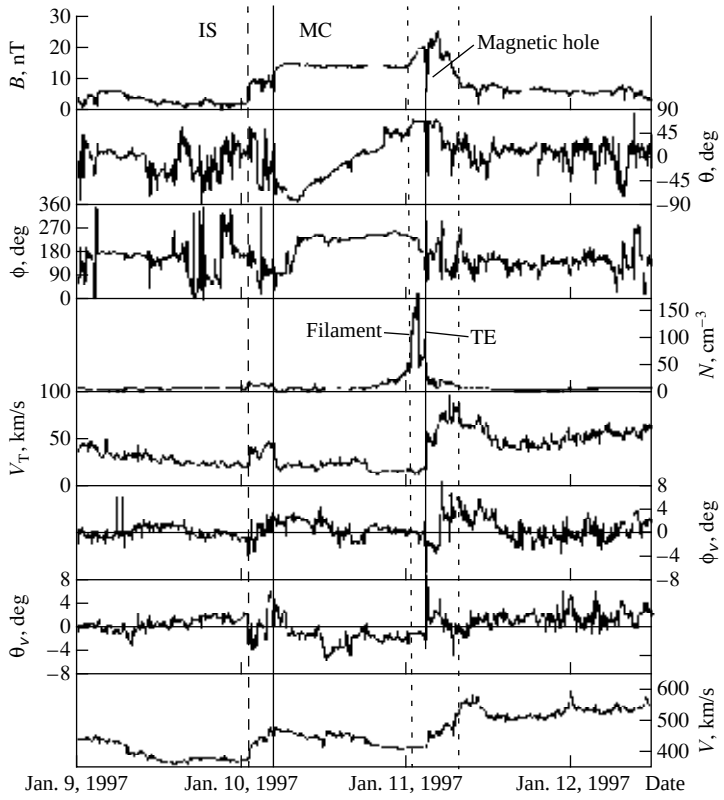

Fig. 1. Plasma and magnetic field parameters in the magnetic cloud on January 10–11, 1997, from observations on the *WIND* satellite: three upper panels represent, respectively, the magnitude and two angles of the magnetic field; next follow the density and thermal velocity; the last three panels show two angles and the magnitude of the bulk velocity.

jumps on leading and trailing edges of MC), and distinctive features (the magnetic "hole" and extremely high density on TE associated with the solar photospheric filament).

As many as 30 magnetic clouds observed during 1995–1998 were included in the analysis. A part of them was analyzed earlier [8], another part was added from the list of coronal mass ejections [10], and a part was taken from the analysis of solar wind and magnetospheric parameters. The list of considered events is presented in Table 1, which includes the date and duration of MC observation (the interval between MC IS and LE is indicated additionally in brackets). Also indicated here are the regions of space, which are crossed at this time by the INTERBALL *Tail Probe* (*INTERBALL-1* hereafter) satellite: SW is the solar wind, MSH is the magnetosheath (the region between the bow shock and magnetopause), MS is the magnetosphere (the tail lobes, plasma and neutral sheets, low- and high-latitude boundary layers).

As is seen from Table 1, the *INTERBALL-1* satellite in the majority of cases was in different regions of the magnetosphere and measured the parameters of plasma, magnetic field, and high-energy particles there. The INTERBALL *Auroral Probe* (*INTERBALL-2*) satellite with a low-apogee 6-h orbit measured various parameters in the polar magnetosphere. Owing to a variety of satellite locations at times of arrival of different MC regions, we have a possibility of investigating the behavior of different magnetosphere regions under different conditions in the SW.

The time dependence of hydrodynamic parameters of plasma and interplanetary magnetic field, observed during the period of lowest SW density on the *WIND* spacecraft, is presented in Fig. 2. The upper panel of Fig. 2 also shows the density measured by the *INTERBALL-1* satellite. We multiplied these density values by a factor of 10 to distinguish them from the *WIND* satellite data. The drop of density caused a considerable increase of the magnetopause and bow shock size, and, since the *INTERBALL-1* satellite was located closer to the Earth than the *WIND* spacecraft, the bow shock sequentially passed by both the satellites in one direction and then backwards (the moments of bow shock crossing by satellites are indicated by BS signs in the upper panel of Fig. 2). In these cases, the satellites entered the magnetosheath for some time. As compared to standard magnitudes of the SW velocity and IMF, the plasma density highly drops and reaches a value lower than 0.2 cm^{-3} at 16:00 UT on May 11, 1999. Though there are some discrepancies in density estimates corresponding to observations on different spacecraft, nevertheless, even for a maximum estimate the density drop exceeds the average value of 8–10 cm^{-3} by a factor of more than 20.

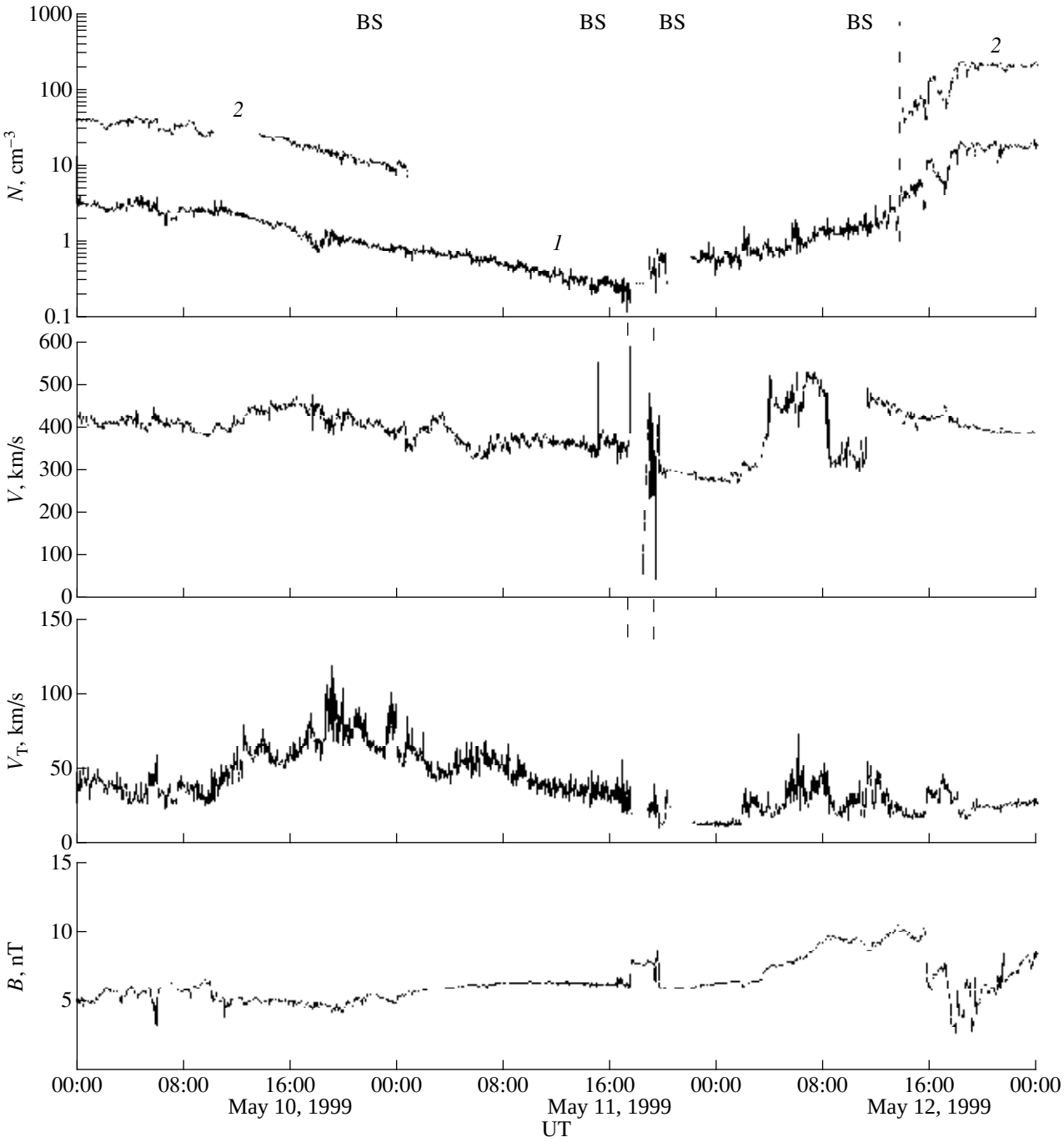

Fig. 2. Plasma and magnetic field parameters in the solar wind with very low density on May 10–12, 1999, from observations on the *WIND* (curve *1*) and *INTERBALL-1* (curve *2*) satellites; the panels from the top to bottom represent the density (the *INTERBALL-1* data are multiplied by 10), bulk and thermal velocities, magnetic field magnitude.

GEOEFFICIENCY OF SOLAR WIND PHENOMENA

The magnetosphere disturbance level can be evaluated on the basis of geomagnetic indices determined from measurements at ground magnetometric stations. For estimating the development of a large-scale storm we used the D_{st} index that describes the geomagnetic field near the equator and a disturbance of the ring current. The D_{st} index variation for the MC on January 10–11, 1997, is shown in Fig. 3. Apparently, we have observed here the sequence of two storms, since, during the interval under consideration, the index has two dips to the negative region: at the beginning of January 10

and at the beginning of January 11, 1997; but the second decrease of the index was weaker. The D_{st} index varies rather slowly, and the main phase of the magnetic storm (the D_{st} minimum is ~ –75 nT) is reached in about 5.5 h after the arrival of MC LE, or in about 9 h after the arrival of IS. The magnetic storm duration (at least till the D_{st} increase up to positive values at the beginning of January 11) is about a day, i.e., it is comparable with the duration of the whole MC; therefore, strictly speaking, the magnetic storm cannot be compared with any MC structure.

To describe the polar region disturbance we have used either the magnetometric records of particular polar stations, near which one or another event took place, or the integral indices (in particular, *Contracted Oval*, *Standard Oval*, and *Expanded Oval*), calculated for three systems of stations located on three concentric circles near the northern magnetic pole (for more details, see the Auroral Oval Indices on the Cluster/Ground-Based Data Center web site http://www.wdc.rl.ac.uk/gbdc/ovals/plots/). The analysis of additional data indicates that these indices are sensitive to substorms and allow one to select them. However, in a small number of cases these indices demonstrate the activations, which are not substorms. In our analysis, we call all these phenomena "activations," having in mind that about 2/3 of the cases relate to substorms. Figure 4 shows these indices for the magnetic cloud of January 10–11, 1997. The comparison of Figs. 1 and 4 indicates that the dips in indices are observed in a few minutes after the arrival of IS and MC LE. However, the changes in the IMF orientation, and jumps in the field strength and SW pressure can be found not for all activations. This comparison of polar indices variations with MC structures was carried out for all MCs shown in Table 1.

Table 2 presents the minimum of hourly average values of the D_{st} index and the number of activations of polar indices related to the number of MC structures. For the event of January 10, 1997, both IS and MC LE correspond to activations (this is designated as 1 activation per 1 structure, or 1/1), while no activations correspond to MC TE on January 11, 1997 (this is designated as 0/1). The decreases of the D_{st} index were observed usually for MCs. However, in some cases (for example, on September 21, 1997, and on June 24–25, 1998) the index pointed to very weak magnetic storms or even their full absence (on June 2, 1998).

The comparison of activations with the MC structure has shown that only 136 of 171 activations (79% of their total number) can be associated with IS before MC LE (IS1), LE, TE, IS in front of TE (IS2), the sign of the B_z component of IMF ($B_z < 0$), and the jumps of the field (ΔB_z) and dynamic pressure of solar wind plasma (ΔP). In this case, the highest relative frequency of activations (the ratio of the number of activations to the number of events of a given type) is observed after IS1 and LE. However, some strong jumps of P and IMF

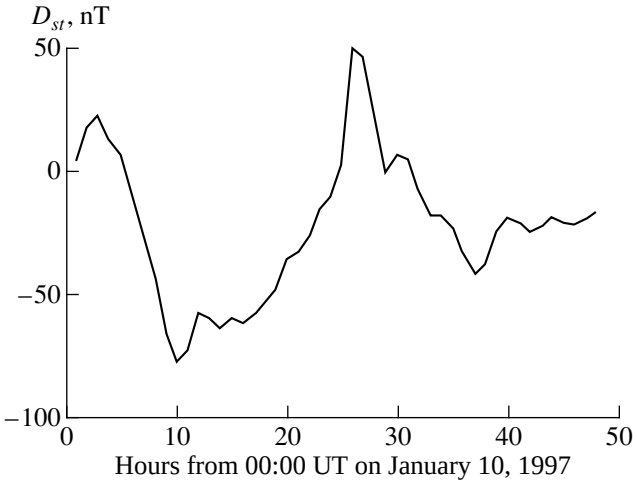

Fig. 3. Time dependence of the global index of geomagnetic activity D_{st} for the magnetic cloud arrival interval on January 10–11, 1997.

(as, for example, a very high pressure jump at MC TE on January 11, 1997) have not resulted in activations. It should be noted that the latter jump was observed after about eight hours of positive B_z component of IMF. Note also that the event on May 10–12, 1999 did not cause any noticeable changes in D_{st} or in polar indices (not shown here).

The data of Table 2 and Fig. 5, constructed on the basis of these data, allow us to assume that there exists some relation between the number of activations N_{ac} and the D_{st} index. Despite a high scatter of the data at a rather scarce statistics, it can be noted that the arrival of MC causing noticeable decrease of D_{st} is accompanied by a higher number of activations (the linear approximation gives the following dependence for the number of activations $N_{ac} = -0.04D_{st} + 2.5$). The question about the relation between slowly varying global geomagnetic indices and rapidly varying polar indices was already discussed in the literature (see, e.g., [2]). However, the mechanisms of such a relation during MC arrival periods can have some peculiarities and require further investigations.

BOUNDARIES OF THE MAGNETOSPHERE

Since the location of the magnetopause (MP) is determined by the balance of plasma and magnetic field pressures in the solar wind, decelerated and heated-up at the bow shock (BS), and inside the magnetosphere, any change of conditions in the interplanetary medium results in a displacement of the MP and, hence, in a displacement of the BS, for which MP is an obstacle when the solar wind flows around it. The *INTERBALL-1* satellite locations at BS and MP crossing times allow the BS and MP locations to be compared with the solar

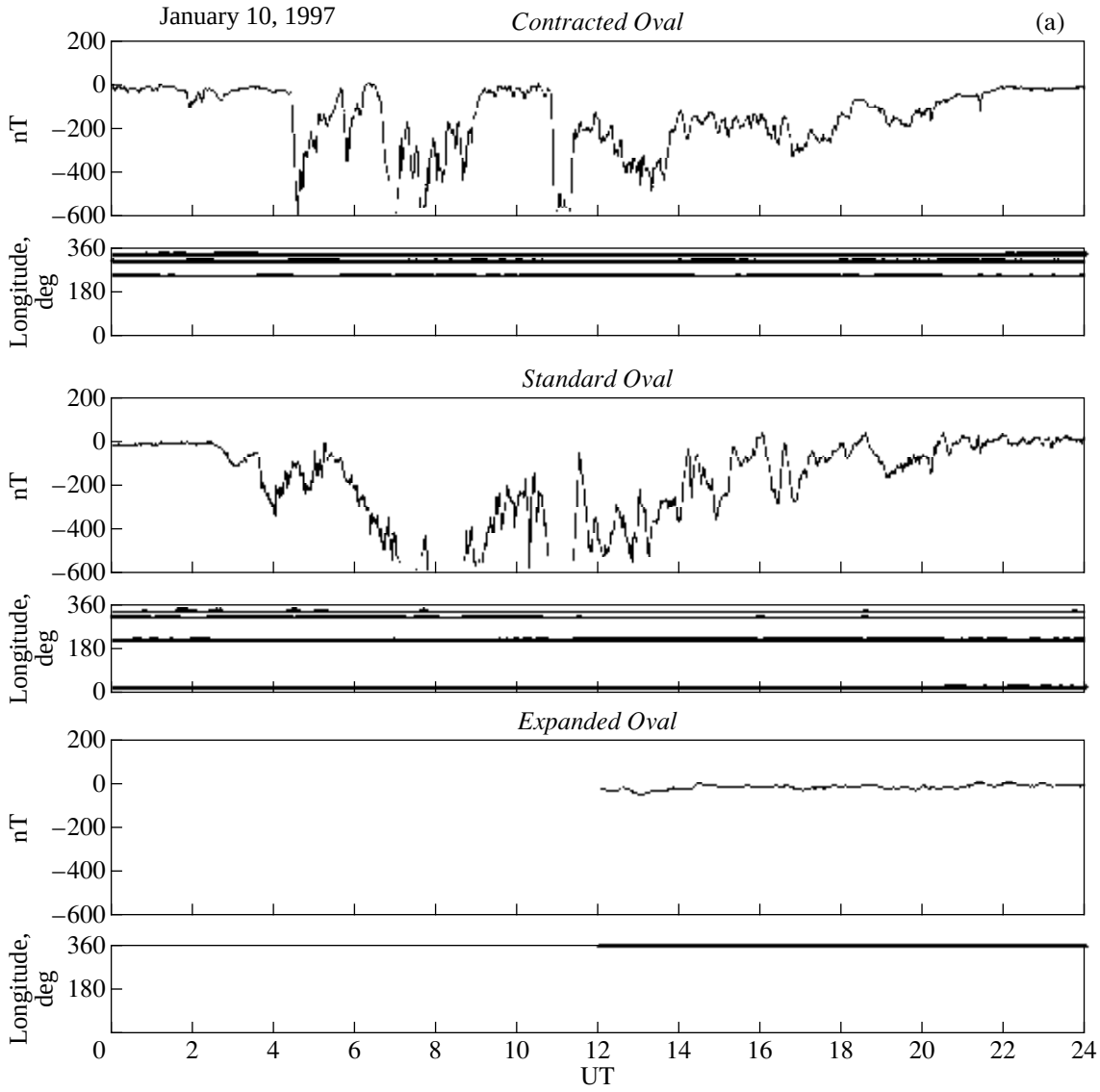

Fig. 4. (a) Time dependence of the auroral indices of geomagnetic activity *Contracted Oval*, *Standard Oval*, and *Expanded Oval* for the magnetic cloud arrival time on January 10, 1997; (b) time dependence of the auroral indices of geomagnetic activity *Contracted Oval*, *Standard Oval*, and *Expanded Oval* for the magnetic cloud arrival time on January 11, 1997.

wind conditions determined by other spacecraft (*WIND, SOHO, IMP-8*) and with model predictions.

We considered 35 MP crossings by the *INTERBALL-1* satellite at MC arrival times. Figures 6a and 6b present the locations of these crossings in the meridional plane (XR_{yz}, where $R_{yz} = \sqrt{Y^2 + Z^2}$) and at the cross-section of the tail (YZ), as well as the average locations of MP and BS. It is seen from the figure that the deviation of a real MP location from average one (observed at an SW pressure of $P \sim 2$ nPa) varies from 1–2 R_E on the MS dayside up to 5–7 R_E in the tail region; in this case, the real MP more often occurs to be closer to the Earth than the average location predicted by the model.

SW parameters (the pressure P and the B_z IMF component) were determined for each MP crossing with taking into account the time lag of plasma propagation between two spacecraft. The range of variation of these parameters for MCs under consideration was found to be wide enough: $0.3 < P < 42$ nPa and $-21 < B_z < 21$ nT. The existing MP models [11–15] have essentially narrower range of variation. The last version of the MP model by Shue *et al.* (1998) [16] was obtained with regard to higher values of SW parameters. By this reason, we have compared the real MP locations with two models, and Fig. 7 presents the distance between the measured location and those predicted in the models by Shue *et al.* (1997) [15] (circles) and Shue *et al.* (1998) [16] (diamonds). In this case, positive distances correspond

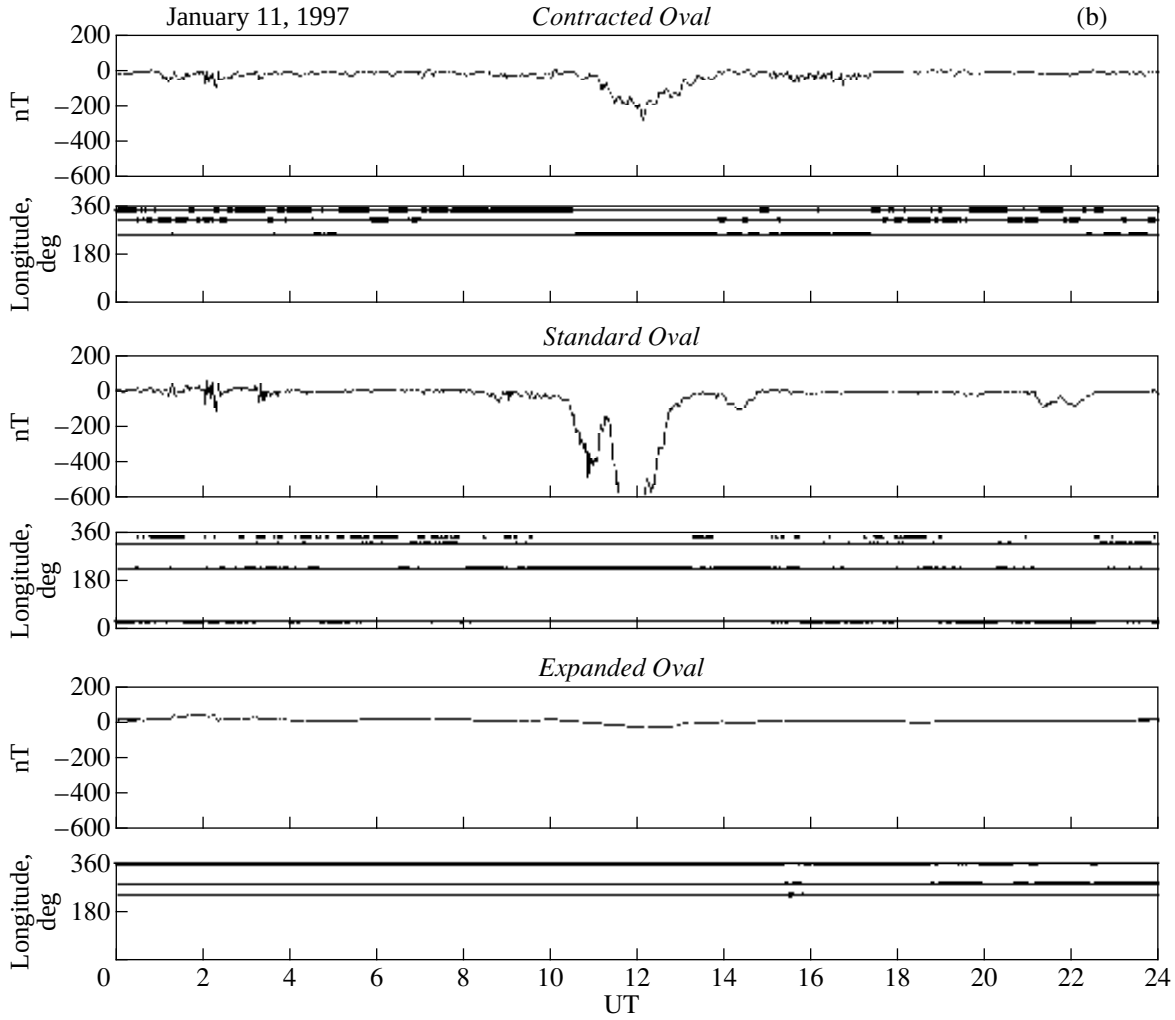

Fig. 4. (Contd.)

to the case, when the measured boundary lies inside model predictions (i.e., closer to the Earth). The distance was measured along the normal to the model boundary.

Figure 7 clearly demonstrates that both the models well predict the MP location in the subsolar region (at $X \geq 0$) and worse in the tail ($X < 0$): on the dayside the MP is located by 1–2 R_E closer to the Earth, and in the tail the scatter is from –5 to +2 R_E. Our statistics does not allow us to compare quantitatively both models with sufficient reliability. However, the large scatter of the real MP location with respect to model predictions testifies that the MP motion during MC arrival is more complicated, than it is predicted by empirical models, which were mainly constructed for the conditions of weakly disturbed SW.

Table 3 presents the results of comparison of the MP location with predictions of the model by Shue *et al.* (1998) [16], as well as the comparison of BS instantaneous location with its average location. Similar statis-

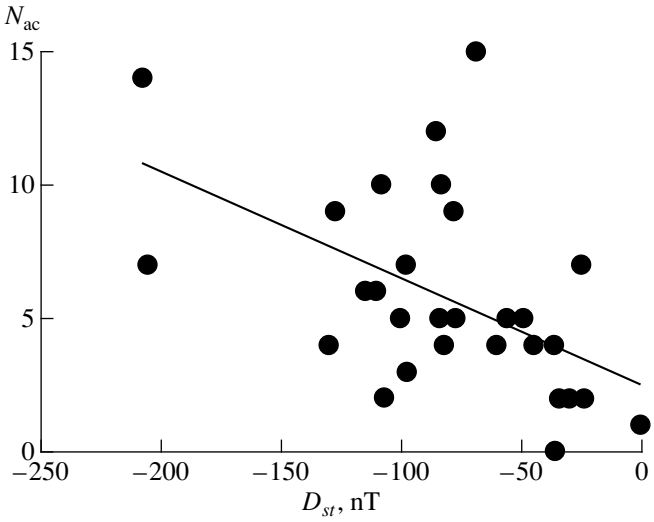

Fig. 5. Observed values of the number of activations N_{ac} and minimum value of D_{st} for magnetic cloud arrival periods.

Table 2. Geoefficiency of magnetic clouds and their structures

Date	D_{st}, nT	Number of substorms and activations							
		Total	IS1	LE	ΔB_z	$B_z < 0$	ΔP	IS2	TE
1995									
Oct. 18–19	–127	9	1/1	1/1	1/1	2	1/3	1/1	0/1
1996									
Dec. 23–25	–33	2	0/1	0/1	0/5	1	1/1	0/0	0/1
1997									
Jan. 10–11	–78	9	0/1	1/1	2/3	2	1/3	0/1	0/1
Feb. 8–11	–68	15	1/1	1/1	2/4	3	3/5	0/0	1/1
Apr. 10–11	–82	4	0/1	1/1	1/2	0	0/0	0/0	1/1
Apr. 21–23	–107	2	1/1	0/1	0/5	0	1/1	0/0	0/0
May 15–16	–115	6	0/1	1/1	2/6	3	0/1	0/0	1/1
June 8–9	–84	5	1/1	0/1	0/5	0	1/6	0/0	0/0
June 19	–36	0	0/1	0/1	0/0	0	0/0	0/0	0/0
July 15–16	–45	4	0/1	1/1	0/0	3	0/0	0/0	0/0
Aug. 3–4	–49	5	0/0	1/1	1/1	0	1/1	0/0	0/1
Sept. 2–3	–98	3	0/1	1/1	0/0	0	1/2	0/0	1/1
Sept. 18–20	–56	5	1/1	0/1	1/3	0	1/3	0/0	1/1
Sept. 21	–24	2	0/1	1/1	0/1	0	0/3	0/0	1/1
Sept. 21–22	–30	2	1/1	1/1	0/0	0	0/1	0/0	0/1
Oct. 1–2	–98	7	1/1	1/1	1/1	0	1/2	0/0	0/1
Oct. 10–12	–130	4	1/1	1/1	1/2	1	0/2	0/0	0/1
Nov. 7–8	–110	6	1/1	1/1	1/3	2	0/1	0/0	0/1
Nov. 22–23	–108	10	1/1	1/1	1/1	6	0/1	0/0	1/1
Dec. 10–1	–60	4	0/1	1/1	1/3	1	0/0	0/0	1/1
Dec. 30–31	–77	5	0/1	1/1	1/1	3	0/0	0/1	0/1
1998									
Jan. 7–8	–83	10	0/1	1/1	4/6	0	0/1	0/0	0/1
Feb. 4–5	–34	2	1/1	0/1	0/0	0	0/6	0/0	0/1
Feb. 17–18	–100	5	0/1	1/1	1/1	1	0/0	1/1	0/1
Mar. 4–5	–36	4	1/1	0/1	2/6	1	0/0	0/0	0/1
May 2–3	–85	12	1/1	1/1	0/3	8	0/1	1/1	0/0
May 4–5	–205	7	1/1	0/1	1/3	1	0/0	0/0	0/1
June 2	–1	1	0/0	1/1	0/1	0	0/0	0/0	0/1
June 24–25	–25	7	0/1	1/1	0/4	5	2/6	0/1	0/1
Sept. 25–26	–207	14	1/1	1/1	1/2	6	0/1	0/0	1/1
Total	–	171	15/28	22/30	25/73	49	14/51	3/6	8/25
Average	–80	5.7							

Table 3. Location of magnetospheric boundaries

Date	Distance* (R_E) between the *INTERBALL-1* satellite and		Date	Distance* (R_E) between the *INTERBALL-1* satellite and	
	bow shock	magnetopause		bow shock	magnetopause
1995			July 3	–2 … –4	–
Oct. 18	–	–2.4 … 1.4	July 4	2	–
Oct. 19	–	–4.4 … 0.6	Sept. 3	2	1.0 … 2.8
1996			Sept. 18	7	–3.5
Dec. 25	~5		Sept. 20	7	–
1997			Sept. 21	7	–
Jan. 10	–	–0.9 … 1.4	1998		
Jan. 11	–	0.0 … 1.5	Feb. 3	–	–0.9
Feb. 8	3	–	Feb. 4	–	–4.7 … –2.0
Feb. 9	2–3	–	Feb. 18	–	1.7
Feb. 10	4	–3.2	Mar. 4	–3 … 3	3.5
Feb. 11	3–6	–	Mar. 5	3 … 4	1.0
June 9	–5 … –6	–0.5	May 4	0	1.7

* Distance is positive, if the boundary is located closer to the Earth than the model boundary.

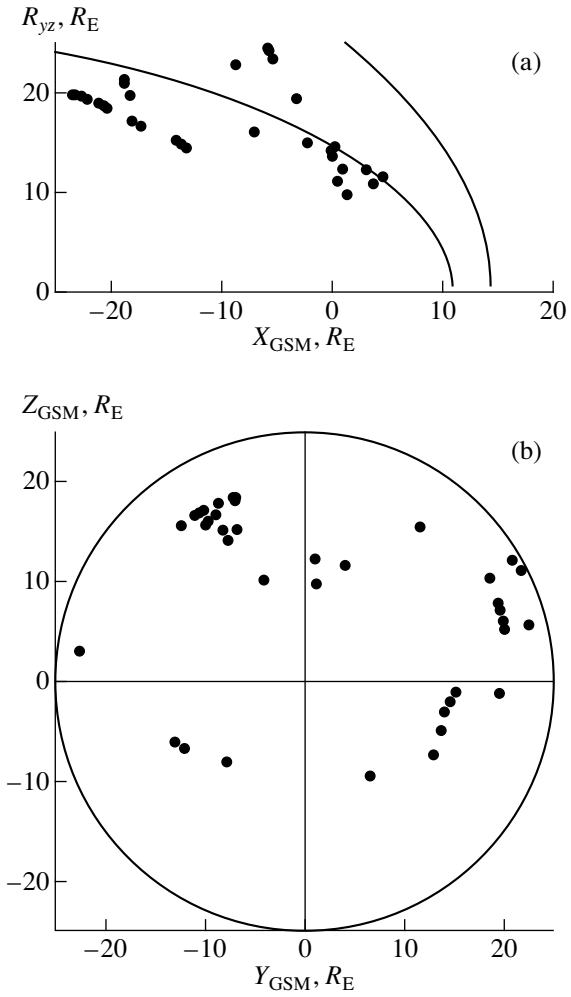

Fig. 6. Magnetopause locations according to observations on the *INTERBALL-1* satellite during the magnetic cloud arrival time in the plane XR_{yz} (a) and in the plane *YZ* (b).

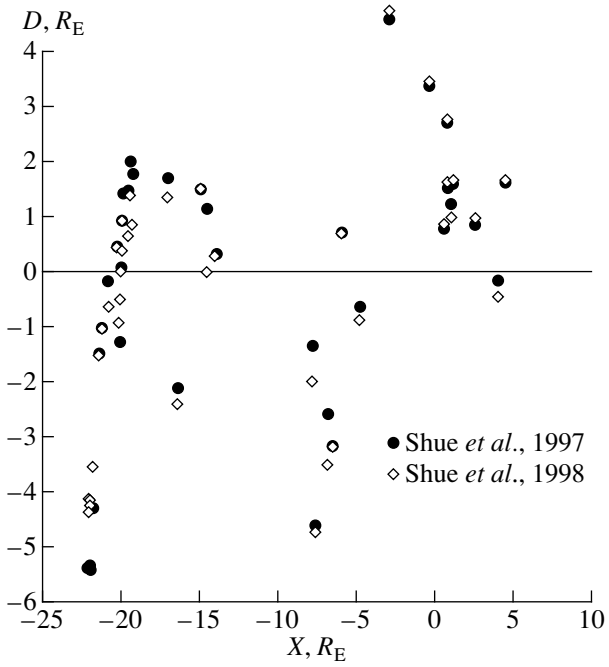

Fig. 7. Comparison of measured magnetopause locations with the models [15] (circles) and [16] (diamonds). The positive distance corresponds to the case, when the magnetopause is located closer to the Earth than predicted by the model.

tical models, taking into account the conditions in the interplanetary space, are not available; by this reason, the real BS location was compared with the average one. However, since the MP is an obstacle for SW in forming BS, we plan to take into account the MP motion depending on conditions in the SW and to investigate the correlation between changes of BS and MP locations. Now we can only notice that the scatter of BS location with respect to average one is approximately the same, as that for MP.

The shape and motion of MP for MC of January 10–11, 1997, were studied, in particular, in papers [17, 18]. The obtained results indicate that the change of MS size was accompanied by more complicated deformations than a simple compression, when different parts of the MS simultaneously undergo proportional displacement, by surface waves on the boundaries and by oscillations of the tail [6, 17]. More complicated character of MS compression follows also from observations on October 18–19, 1995, since these data were interpreted as a consequence of reconnection of magnetic field lines not in the subsolar region or near the cusp, but rather on the MP in the far tail at distances $|X|$ larger than 20 R_E [19].

The black diamonds in Fig. 8 show the location of the *INTERBALL-1* (*I-1*), *WIND* and *GEOTAIL* (*GE*) satellites on May 10–12, 1999, when they were crossing the BS. The empty diamonds in this figure show the BS location predicted by the model [21] for conditions in the solar wind at the time of BS crossing by a corresponding satellite. The curves present the results of calculations by models [20] (curve *1* for P = 0.08 nPa; curve *2* for P = 0.50 nPa) and [21] (curve *3* for P = 2.0 nPa). The decrease of solar wind density on May 10–12, 1999, resulted in a noticeable expansion of the MS. In this case, according to the *WIND* spacecraft data, the BS was displaced outwards to such a distance, that at the minimum SW density time the subsolar BS point was situated at the distance from the Earth larger than 45 R_E, its average location being about 15 R_E. According to the *INTERBALL-1* satellite data, a few hours earlier the BS was observed at a distance of about 16 R_E (reduced to the subsolar point). The models used, which were constructed three decades ago, unsatisfactorily describe the BS location, especially under the conditions of very low solar wind density, and require further improvement.

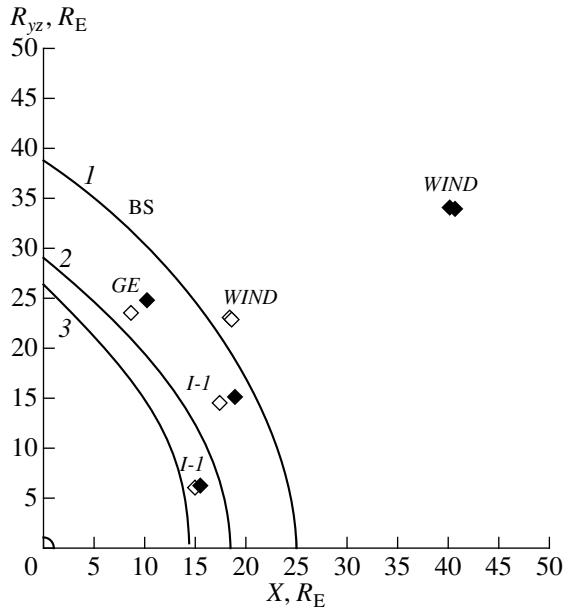

Fig. 8. The Earth's bow shock location for the interval of arrival of the solar wind with very low density on May 10–12, 1999 according to observations on the *INTERBALL-1* (*I-1*), *WIND*, *GEOTAIL* (*GE*) spacecraft and model calculations [20, 21] (see text).

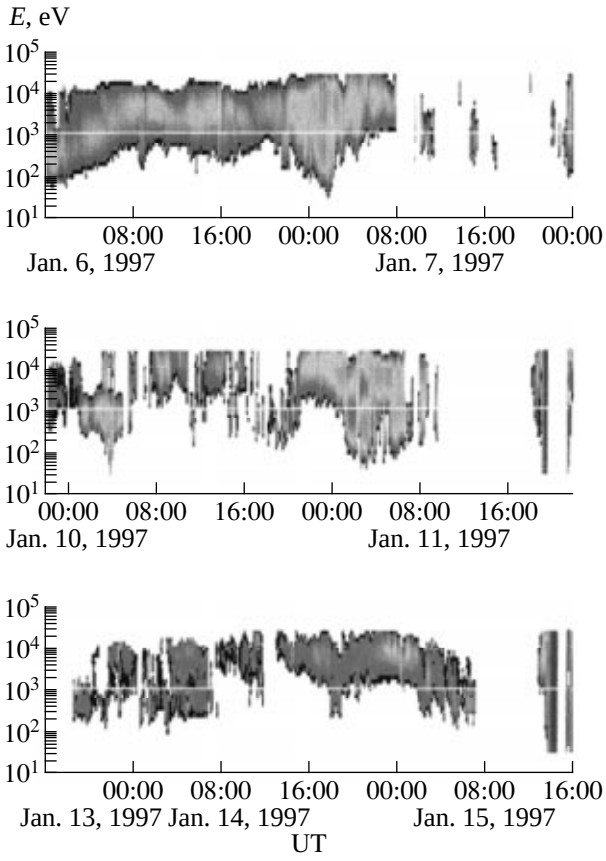

Fig. 9. Variation of the energy spectrogram of ions during 3 successive orbits of the *INTERBALL-1* satellite on January 5–15, 1997.

STATE OF THE MAGNETOSPHERE

As it was shown in previous section, the MC arrival to the Earth is accompanied by the displacement of MS boundaries. This implies, in particular, that the place, where one physical region of space is usually observed (which is characterized by typical values of plasma and magnetic field parameters), occurs to be occupied by an absolutely different region, which is observed far from this place under normal conditions. And though small displacements of various types of regions is a rather frequent phenomenon in such a dynamic system as the MS, displacements to distances comparable with the size of regions or even greater are quite rare phenomena. This fact should be taken into account when comparing the parameters of usual magnetosheath (for instance) with those of magnetosheath-like plasma, which is observed in the region, where the plasma sheet is usually observed. On the other hand, such an analysis is very important, since it provides the additional information on the dynamics and mechanisms of formation of different MS regions. We have considered only some examples from a large set of various cases of anomalous location of MS regions, and the results presented below (which have been partially published in papers [6–8]) can be considered only as a first step in this direction.

Figure 9 shows the dynamic energy spectrograms of ions (the abscissa is time, the ordinate is energy; the color from black to gray indicates increasing value of the ion flux) for three successive orbits of the *INTERBALL-1* satellite during the period of January 5–15, 1997. In this case, the data, placed on the same vertical straight line, were obtained, approximately, at the same satellite coordinates. (Due to the annual satellite orbit evolution with respect to the Sun–Earth axis the planes of successive orbits occur to be displaced relative to each other by an angle of about ~4°.) These data represent the ion energy spectrograms obtained by the CORALL instrument with the help of a sensor oriented perpendicular to the satellite's spin axis (i.e., in the plane normal to the Sun–Earth line).

The upper panel, whose data were obtained before the MC arrival, shows at first a hot and rarefied plasma of the plasma sheet. In the time interval from 22 UT on January 6 to 02 UT on January 7, when the satellite was close to the geomagnetic equator ($X \sim -17$ and $Y_{GSM} \sim 16R_E$), the plasma of a low-latitude boundary layer (LLBL) was observed. After this, the satellite began to approach the Earth, while crossing several times the regions of plasma mantle and the tail lobes, and at ~23 UT the satellite reached the radiation belt.

Before the MC arrival on January 10 the plasma sheet's plasma, more precisely, PSBL (the plasma sheet boundary layer on the PS outer part) was observed. However, at about 01:20 UT the satellite crossed the MP and occurred to be in the magnetosheath. Then, from ~06 to ~20 UT, the instrument recorded both long (for ~1–2 h) intervals and short (a few minutes) bursts

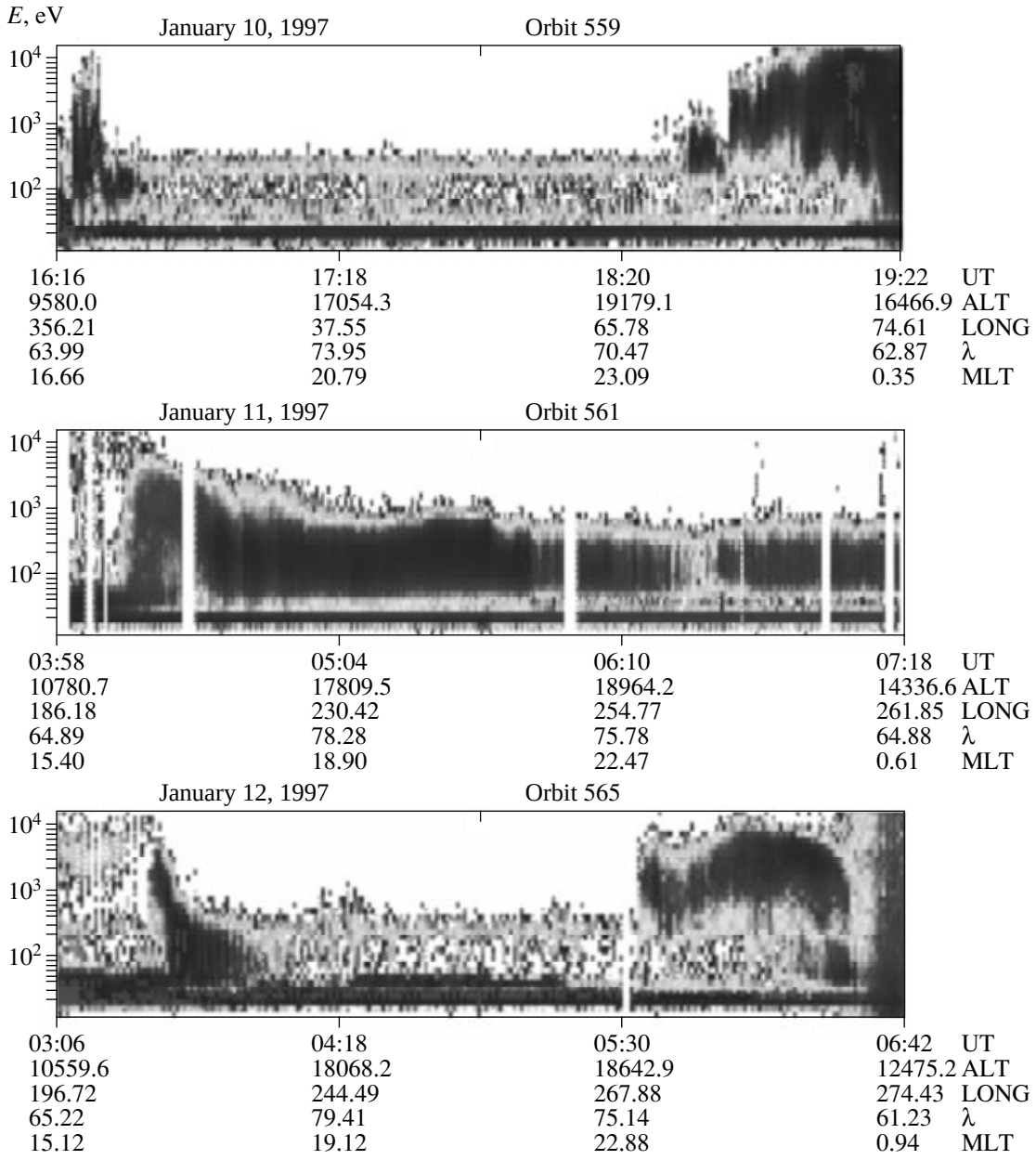

Fig. 10. Variation of the energy spectrogram of electrons during 3 orbits of the *INTERBALL-2* satellite on January 10–12, 1997.

of the plasma sheet with lower density and higher energy than on a previous orbit. The plasma sheet observations were interrupted by satellite exit to the lobes, which testifies to fast motions of the geomagnetic tail with respect to a rather slowly moving satellite. After MC TE arrival at ~01:20 UT on January 11, the satellite from the plasma sheet quickly entered a very dense and hot magnetosheath, then, at ~02 UT, it could be found in the LLBL (at a rather large distance from the geomagnetic equator, $Z_{GSM} \sim 8$–$9R_E$) and then in the plasma sheet.

The plasma sheet parameters, observed on January 13–14, had intermediate values between those observed before and during MC arrival; in this case, the geomagnetic tail continued to be noticeably displaced relative to the satellite.

The dynamic energy spectrograms of electrons, measured by the ION instrument on subsequent orbits of the *INTERBALL-2* satellite, are presented in Fig. 10. Before the MC arrival, in the polar cap (invariant latitude $\lambda > 65°$) the fluxes of electrons had too low energy of several tens of electronvolts and too low intensity to be observed. However, after the MC TE arrival on January 11, 1997, high fluxes of electrons with an energy of 100–300 eV were detected in the polar cap. This period coincides with the *INTERBALL-1* satellite exit

from the plasma sheet into the magnetosheath and LLBL, i.e., the disturbance of a far tail of MS coincided with electron precipitation in the polar cap.

Thus, the peculiar features of the magnetosheath and magnetosphere plasma observed during the MC arrival, can now be summarized as follows.

—The observation of very hot (on January 10–11, 1997, for instance [6, 7]) as well as very cold (on October 19, 1995 [19]) plasma in the magnetosheath.

—A very dense ($N \sim 150$ cm^{-3}) plasma in the magnetosheath [17] and no correlations between simultaneous values of density in the magnetosheath and in the plasma sheet [6, 7].

—The observation of plasma of the LLBL type at a large distance ($8\,R_E$) from the geomagnetic equator [6, 7].

—The geomagnetic tail oscillations relative to a satellite, so that the displacements of some regions are comparable to characteristic dimensions of a given region [6–8].

—The development of disturbances and acceleration of ions and electrons in the plasma sheet, their subsequent injection and precipitation in polar regions of the magnetosphere [6, 8].

—A global decrease of the plasma density in different magnetospheric regions at the "weak" solar wind time on January 10–12, 1999.

DISCUSSION AND CONCLUSIONS

Presented results of the analysis of magnetic clouds and "weak" solar wind interaction with the Earth's magnetosphere, based on the *INTERBALL-1*, and *INTERBALL-2* satellite data, allow us to make some conclusions about the magnetosphere response to such effects.

The geoefficiency of magnetic clouds, apparently, depends on the value of variation of parameters in the magnetic cloud. For low, medium, or moderately high variations of plasma and magnetic field parameters in a cloud, the magnetosphere response is the same, as for similar variations in the interplanetary space in the absence of magnetic clouds, and strongly depends on the interplanetary magnetic field prehistory:

—after prolonged energy transfer to the magnetosphere (at the southward IMF orientation), virtually all changes in the solar wind pressure or in the IMF magnitude and orientation can result in auroral activations, substorms, and magnetic storms;

—at a prolonged northward orientation of the IMF, virtually all changes of magnetic cloud parameters are not geoeffective and do not have noticeable influence on the state of the magnetosphere and on the geomagnetic field.

Extremely high jumps of parameters in magnetic clouds (mainly, near their boundaries, in shock waves, at leading and trailing edges) can result in the unusual behavior of the magnetosphere, namely:

—strong and rather complicated compression and deformation (with large and disproportional displacement of boundaries) of the magnetosphere relative to its usual location;

—large-scale oscillations of geomagnetic tail structures relative to a satellite;

—the development of disturbances in the plasma sheet, which result in acceleration of ions and electrons and their injections in the polar cap region.

The magnetic clouds, causing a great number of polar disturbances including substorms, are accompanied, as a rule, by stronger global disturbances like magnetic storms.

The event with a strong density decrease in the solar wind on January 10–12, 1999, did not cause any noticeable change of geomagnetic indices, though a high increase of the magnetosphere size was observed in this case.

The Earth's magnetosphere behavior under extreme conditions in the interplanetary medium, observed at arrivals of magnetic clouds, poorly agrees with available statistical models, is insufficiently studied yet, and requires further investigations.

ACKNOWLEDGMENTS

This work was partially supported by the Russian Foundation for Basic Research, projects nos. 96-15-96723, 97-02-16489, and 98-05-64508, and by the INTAS, grants nos. 96-2346, 97-1612, and 99-0078. The key parameters of plasma and magnetic field in the *WIND* project (principal investigators of experiments K.W. Ogilvie and R.P. Lepping) were obtained from the NASA Goddard Space Flight Center via CDAWeb. The data on Auroral Oval Indices were obtained from the Cluster/Ground-Based Data Center. We thank S.I. Klimov, S.A. Romanov, M.N. Nozdrachev, and A.A. Skalsky for magnetic field measurement results; A.O. Fedorov for his participation in the processing of the CORALL instrument data; J.-A. Sauvaud and R.A. Kovrazhkin for presentation of the ION and ELECTRON instrument data; S.P. Savin, N.L. Borodkova, L.M. Zelenyi, Z. Nemecek, J. Safrankova, and Yu.I. Galperin for assistance and useful remarks; and V.I. Prokhorenko for calculations of *INTERBALL* satellites orbits.

REFERENCES

1. Akasofu, S.-I., Energy Coupling between the Solar Wind and the Magnetosphere, *Planet. Space Sci.*, 1981, vol. 28, p. 121.
2. *Proc. 4th Int. Conf. on Substorms, SUBSTORMS-4*, Kokubun, S. and Kamide, Y., Eds., Terra Sci./Kluwer Academic, 1998.
3. Burlaga, L., Fitzenreiter, R., Lepping, R., *et al.*, A Magnetic Cloud Containing Prominence Material: January 1997, *J. Geophys. Res.*, 1998, vol. 103, p. 277.

4. Webb, D.F., Coronal Mass Ejections: The Key to Major Interplanetary and Geomagnetic Disturbances, *Rev. Geophys., Suppl.*, 1995, p. 577.
5. Gosling, J.T., McComas, D.J., Phillips, J.L., *et al.*, Geomagnetic Activity Associated with Earth Passage of Interplanetary Shock Disturbances and Coronal Mass Ejections, *J. Geophys. Res.*, 1991, vol. 96, p. 7831.
6. Yermolaev, Yu.I., Zastenker, G.N., Borodkova, N.L., *et al.*, Magnetic Cloud Event on 6–11 January, 1997: INTERBALL Multi-Satellite and Multi-Instrument Observations, *Proc. 31st ESLAB Symp. ESA SP-415*, 1997, p. 155.
7. Yermolaev, Yu.I., Zastenker, G.N., Nozdrachev, M.N., *et al.*, Plasma Populations in the Magnetosphere during the Passage of Magnetic Cloud on 10–11 January, 1997: INTERBALL/*Tail Probe* Observations, *Geophys. Res. Lett.*, 1998, vol. 25, p. 2565.
8. Yermolaev, Yu.I., Zastenker, G.N., Borodkova, N.L., *et al.*, Statistic Study of Magnetosphere Response to Magnetic Clouds: INTERBALL Multi-Satellite Observations, *Phys. Chem. Earth C*, 2000, vol. 25, p. 177.
9. Le, G., Russell, C.T., and Petrinec, S.M., The Magnetosphere on May 11, 1999, the Day the Solar Wind almost Disappeared: I. Current Systems, *Geophys. Res. Lett.*, 2000, vol. 27, p. 1827.
10. Gopalswamy, N., Lara, A., Lepping, R.P., *et al.*, Interplanetary Acceleration of Coronal Mass Ejections, *Geophys. Res. Lett.*, 2000, vol. 27, p. 145.
11. Sibeck, D.G., Lopez, R.E., and Roelof, E.C., Solar Wind Control of the Magnetopause Shape, Location, and Motion, *J. Geophys. Res. A*, 1991, vol. 96, no. 4, p. 5489.
12. Roelof, E.C. and Sibeck, D.G., Magnetopause Shape as Bivariate Function of Interplanetary Magnetic Field B_z and Solar Wind Dynamic Pressure, *J. Geophys. Res. A*, 1993, vol. 98, no. 12, p. 21421.
13. Petrinec, S.M. and Russell, C.T., Near-Earth Magnetotail Shape and Size as Determined from the Magnetopause Flaring Angle, *J. Geophys. Res.*, 1996, vol. 101, p. 137.
14. Kuznetsov, S.N. and Suvorova, A.N., The Magnetopause Form in the Region of Geosynchronous Orbit, *Geomagn. Aeron.*, 1997, vol. 37, no. 3, p. 1.
15. Shue, J.-H., Chao, J.K., Fu, H.C., *et al.*, A New Functional Form to Study the Solar Wind Control of the Magnetopause Size and Shape, *J. Geophys. Res.*, 1997, vol. 102, no. 5, p. 9497.
16. Shue, J.-H., Song, P., Russell, C.T., *et al.*, Magnetopause Location under Extreme Solar Wind Conditions, *J. Geophys. Res. A*, 1998, vol. 103, no. 8, p. 17691.
17. Nikolaeva, N.S., Zastenker, G.N., Nozdrachev, M.N., *et al.*, Position and Motion of the Magnetopause during arrival of a Magnetic Cloud to the Earth on January 10 and 11, 1997, *Kosm. Issled.*, 1998, vol. 36, no. 6, p. 564.
18. Safrankova, J., Nemecek, Z., Prech, L., *et al.*, The January 10–11, 1997, Magnetic Cloud: Multipoint Measurements, *Geophys. Res. Lett.*, 1998, vol. 25, p. 2545.
19. Savin, S., Balan, O., Borodkova, N., *et al.*, INTERBALL Magnetotail Boundary Case Studies, *Adv. Space Res.*, 1997, vol. 20, no. 4/5, p. 999.
20. Spreiter, J.R., Summers, A.L., and Alksne, A.Y., Hydromagnetic Flow around the Magnetosphere, *Planet. Space Sci.*, 1966, vol. 14, p. 223.
21. Fairfield, D.H., Average and Unusual Location of the Earth's Magnetopause and Bow Shock, *J. Geophys. Res.*, 1971, vol. 76, p. 6700.